ICANS XIX,
19th Meeting on Collaboration of Advanced Neutron Sources
March 8 – 12, 2010
Grindelwald, Switzerland

LIMET- A TEST BED FOR LIQUID METAL TARGETS

SERGEJS DEMENTJEVS
Paul Scherrer Institut
CH-5232 Villigen PSI, Switzerland

and

RADE Ž. MILENKOVIĆ[a], VADIMS GEZA[b], FILIPPO BARBAGALLO[a] , STEFAN JORAY[a], RALF KAPULLA[a], AUGUST KALT[a], ENZO MANFRIN[a], JACEK PATORSKI[a], MICHAEL WOHLMUTHER[a]
[a]*Paul Scherrer Institut, CH-5232 Villigen PSI, Switzerland*
[b]*University of Latvia, Riga, Latvia*

ABSTRACT

As the most delicate component of the lower target container is the Beam Entrance Window (BEW), it is necessary to demonstrate that the structural integrity of the window would be maintained under a variety of operational and accident-scenario conditions. It is of crucial safety importance that the BEW is adequately cooled. In the actual MEGAPIE (Megawatt Pilot Experiment) design, unidirectional flow across the window was affected by a jet exiting from a bypass nozzle in order to provide sufficient window cooling. As the use of an additional bypass pump increased significantly the complexity and costs of the system, the idea of having a reliable configuration without additional bypass flow directed the design efforts.
Therefore, the main objective of the activities, which comprise extensive experimental and computational studies and are coordinated under project LIMET (Liquid Metal Target test bed), is to investigate various designs and cooling capabilities of the lower target region without a using bypass flow nozzle and to analyse hydraulic, structural and thermal behaviour of the target mock-up. The preliminary computations have been performed for water and LBE (Lead Bismuth Eutectic) as working fluids and for various geometrical parameters. The optimization of these geometrical parameters is planned to be achieved by combining experimental investigations with computational studies.
Two experimental series have been planned: water (LIMETW) and liquid metal experiments (LIMETLBE). A goal of the water experiments (LIMETW) is to investigate several geometries of the riser tube end geometries that should provide adequate cooling of the BEW. They will be subsequently investigated during the second session named LIMETLBE.

1. Introduction

As the most delicate component of the lower target container is the Beam Entrance Window (BEW), it is necessary to demonstrate that the structural integrity of the window would be maintained under a variety of operational and accident-scenario conditions. It is of crucial safety importance that the BEW can be adequately cooled. In the actual MEGAPIE design [1] unidirectional flow across the window was affected by a jet exiting from a bypass nozzle in order to provide adequate window cooling. This rectangular nozzle delivered a relatively thin fluid stream for cooling the window, while coolant from the annulus into the target riser and carries heat away up to the target heat exchanger together with the stream cooling the window. As the use of an additional bypass pump increases significantly the complexity and costs of the system, the idea of having a reliable configuration without additional bypass flow directed the design efforts. Therefore, the main motivation for undertaking further research activities is to find a lower target design with a BEW that would be adequately cooled only by the main flow.

The corresponding extensive experimental and computational studies coordinated under the project LIMET (Liquid Metal Target Test bed) comprise the investigation of various designs of the lower target region without using bypass flow and to investigate the hydraulic, structural and thermal behavior of the target mock-up. The computational simulations, which are performed by CFX 11.0, ANSYS and Workbench in the first part of the project, have the goal of designing and optimizing the 3D geometrical layout and investigating its performance and behavior in steady-state operation, without and, later with taking into account heat deposited by the proton beam. The computations are to be performed for water and LBE (Lead Bismuth Eutectic) as working fluids and for various geometrical parameters. The optimization of these geometrical parameters is planned to be achieved by combining experimental investigations with computational studies.

Initial computational studies, which are briefly summarized in Chapter 2, showed very complex 3D flows in the lower target. Therefore, no guaranties for adequate window cooling without bypass flow can be given in advance, and through experimental investigations must be conducted in addition. Two experimental series have been planned: water (LIMETW) and liquid metal experiment (LIMETLBE).

A goal of the water experiments (LIMETW) is to investigate several variants of the riser tube end geometries that should provide adequate cooling of the BEW. They will be subsequently investigated during the second session LIMETLBE. As already mentioned above all planned investigations consist of theoretical and experimental contributions.

The skeleton of the study consists of the following:

-Validation of CFD procedure, which includes calculations of the liquid metal velocity field in the beam entrance window of the reference geometry (see Chapter 3);

-Validation of the CFD calculations by using experimental results from LIMETW tests, in particular PIV velocity- and hydraulic pressure loss-measurements, for the BEW of the reference configuration;

-Development (on the basis of the CFD calculations) of one or several concepts of “promising” geometries of the lower target;

-Experimental investigation of structural and hydraulic behavior of the mock-up: velocity fields; hydraulic pressure loss; cavitation and flow-induced vibrations.

An additional goal of the investigation is the acquiring of experimental experience necessary for a solid target cooling optimization. This includes testing of various experimental techniques and computational procedures. Namely, the same mock-up can be used for testing water-cooled solid-target geometries.

2. Summary of initial computational studies

Fig. 1 shows a conceptual vertical design of the liquid metal target without a bypass. In the MEGAPIE target, adequate cooling of the window was achieved by using a jet flow superimposed on the main annular flow exiting from jet nozzle (not shown here). This additional bypass flow created a steady liquid metal stream over the centre of the beam entrance window (BEW) and moved the flow stagnation point outside of the proton beam. In the current design no bypass flow is considered. Adequate cooling must be achieved by directing the main flow, which performs a U-turn from the annulus to the cylindrical riser tube near BEW. In order to avoid flow stagnation on the BEW, the lower end of the annulus is asymmetrically closed. Only a hemispherical window was considered. In order to provide enough space for thermal expansion of the riser (often called guide tube) during operation (when a large amount of heat is deposited in the target) gaps between the cylindrical part of the hull and the riser tube must be properly sized. If the riser tube with the additional plate does not penetrate into the hemispherical domain of the hull, flow detachment and huge stagnation regions are obtained by the simulations at the centre of the BEW for almost all gap sizes. If the riser tube is shifted down, flow detachment at the hemispherical shell can be avoided, but the thermal expansion constraint poses a problem. Therefore we try the following concept: the annular flow is asymmetrically separated and directed over the BEW by an additional plate called splitter plate. The plate should be wide enough for the jet to cover the region at the window with highest beam deposition and close enough to wall to allow a jet flow to cool convectively the window. Such a plate (and the riser tube) will be exposed to flow-induced vibrations and thermal cycling; therefore it must be carefully designed and tested.

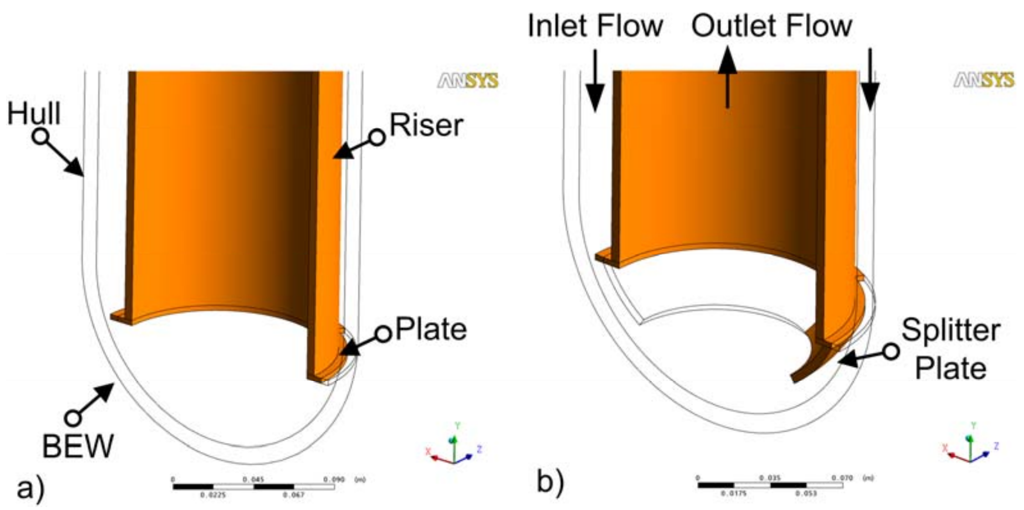

Fig. 1. Detail of the lower target.

The velocity fields obtained from RANS (Random Averaged Navier Stokes) simulations show the complexity of the flow field and its dependence on various geometrical parameters and configurations.

The models are constructed and meshed by using ANSYS ADPL. This approach enables fast and reliable generation of various geometrical models as well as variable mesh refinement close to the solid boundaries. The CFX 11.0 code (RANS) was used to predict velocity fields and pressure loss in the BEW region. A structured mesh with mesh narrowing near solid boundaries was used. Calculations were performed using a three-dimensional model with non-uniform hexahedral meshes refined at all solid no-slip boundaries. All simulations were for steady-state conditions. The three-dimensional CFD models reported here contained between 300,000 and 500,000 cells. The High Resolution Scheme for advection was used.

Regarding turbulence modeling two approaches have been used: the low Reynolds number approach (SST model as combination of and models) and high-Reynolds number $k-\varepsilon$ model. For the first one, the law-of-the-wall representations are automatically used, if the automatic near-wall treatment option in CFX is switched on. The idea behind the automatic near-wall treatment is that the model shifts gradually between a viscous sub-layer formulation (the low Reynolds number approach) and wall functions, based on the grid density. The ω-equation is well suited for this task, as it provides analytical solutions, both for the sub-layer and the logarithmic region. A blending function depending on y^+ can therefore be defined. Here, all y^+ and SST model simulations have been computed with the automatic wall treatment. Basically, it is ensured that the right formulation for wall treatment based on y^+-values is used.

For the high-Reynolds approach y^+-values were kept in the range 30< y^+ <200, so that the wall functions used with $k-\varepsilon$ turbulence model would be valid. Nevertheless, this criterion could not be fulfilled in some regions near flow stagnation so that a small uncertainty remains in the calculation.

In addition, an attempt was made to keep the mesh spacing in the wall-normal direction such that the y^+-values of the near wall nodes were less than 1. In order to resolve properly the distribution of velocity and other variables, approximately 10-15 mesh nodes are placed within the near-wall region. These equations are valid for turbulent boundary layer formed along the flat plate.

The following physical and boundary conditions were implemented:

- fluid: water, physical properties at 20 °C;
- constant mass flow rate at the inlet;
- open boundary condition at the outlet;
- no slip, adiabatic walls;
- no buoyancy;
- flow symmetry with respects to symmetry plane through target axis.

3. Configurations of the riser tube end under investigation

3.1. Configuration A: the reference configuration

The beam entrance window of the reference configuration was designed especially for the validation of the CFD and LES calculations (see Fig. 9). This configuration is not optimal for the window shell cooling but meets the following requirements: simplicity and convenience for fabrication and good accessibility for PIV technique.

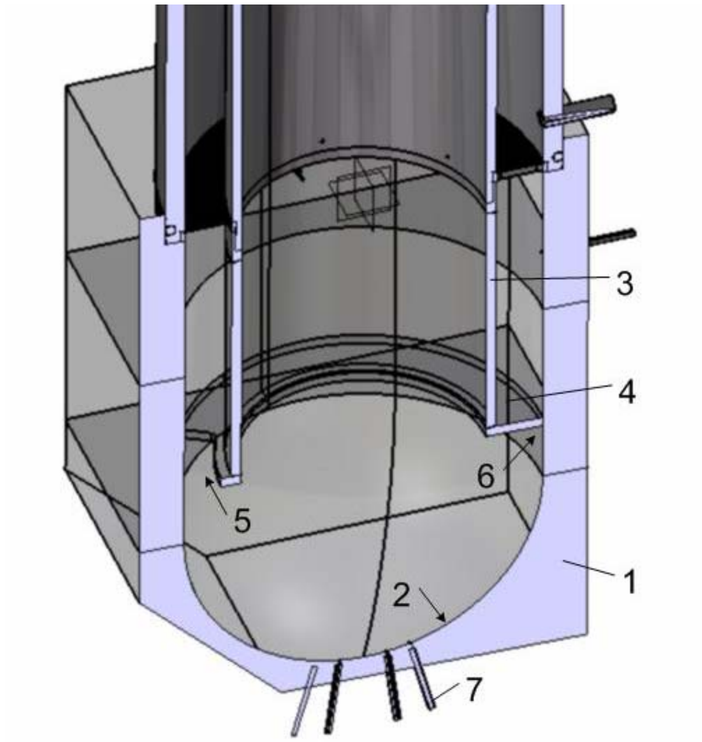

Fig. 2. Lower target mock-up of reference configuration A: 1 – Plexiglas mock-up of BEW; 2 – BEW shell; 3 – riser tube; 4 – riser skirt; 5 – main jet opening; 6 – annular gap for residual flow.

3.2. Configuration B

The BEW configuration B has been designed on the basis of Platnieks proposal (Fig. 3, [4]). A heat transfer enhancement from the window shell depends on the development of a free boundary layer near the shell. Therefore, it can be strongly affected by the geometrical configuration. The distance between the turbulence promoting insert and the hemi-spherical shell of the BEW is considered to play an important role. This will be investigated during the experiments.

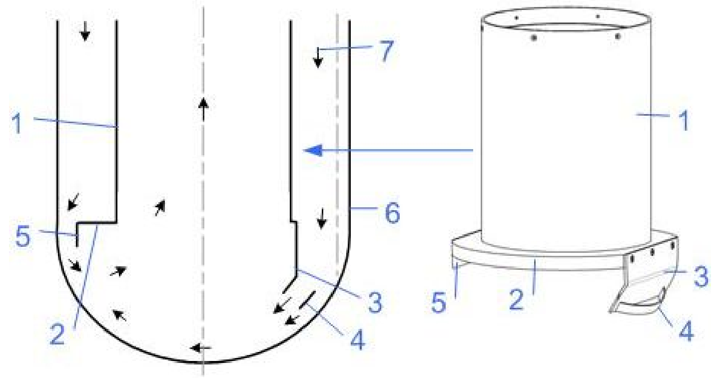

Fig. 3. Riser end of configuration B: 1 – riser tube end; 2 – skirt of the riser tube end; 3 - main jet guide; 4 - turbulence promoting insert; 5 – annular gap; 6 – calotte (mock-up of BEW); 7 – water flow.

3.2. Configuration C

This configuration is presented in Fig. 4a. We consider this version as a candidate for testing with liquid metal. Some further modification and improvements are not excluded. Preliminary computational studies were done and the results for mean velocity fields are presented in Fig. 4 and Fig. 5.

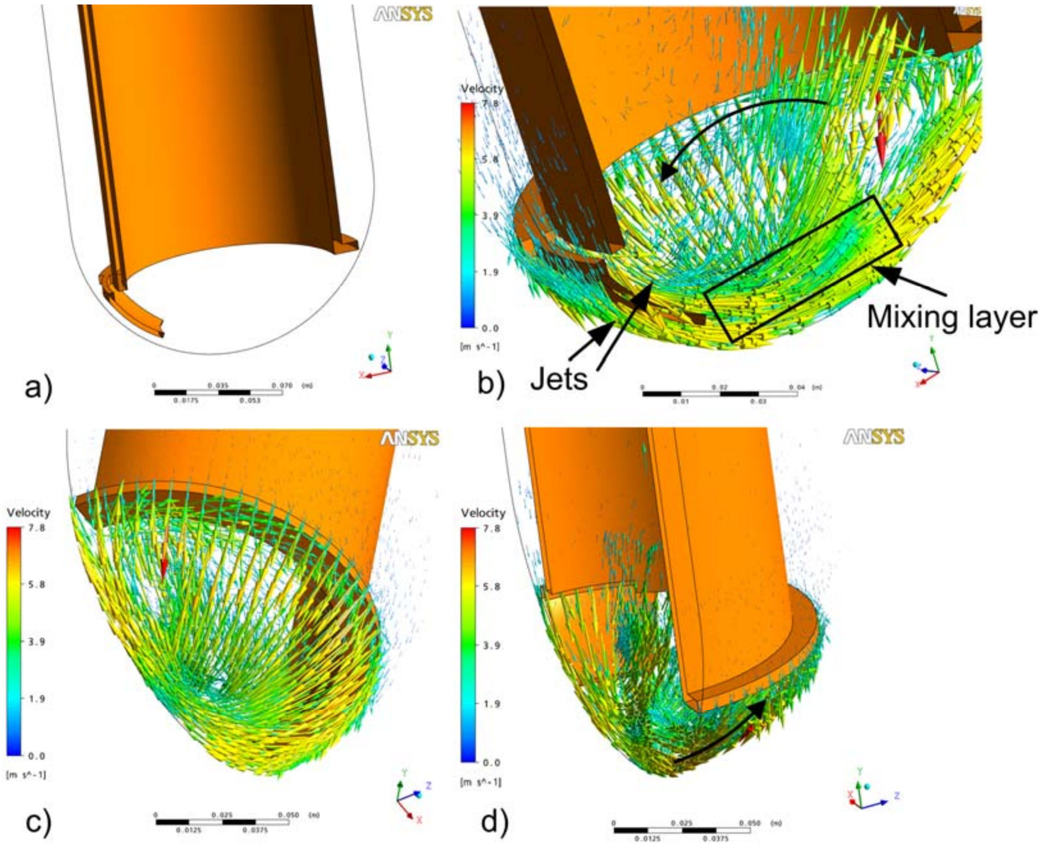

Fig. 4. a) Configuration C; Velocity vectors b) symmetry plane view; c) view from bottom; d) side view reveal complex 3D velocity field near the window as well as inside the riser. Comment: RANS-time averaged velocity fields.

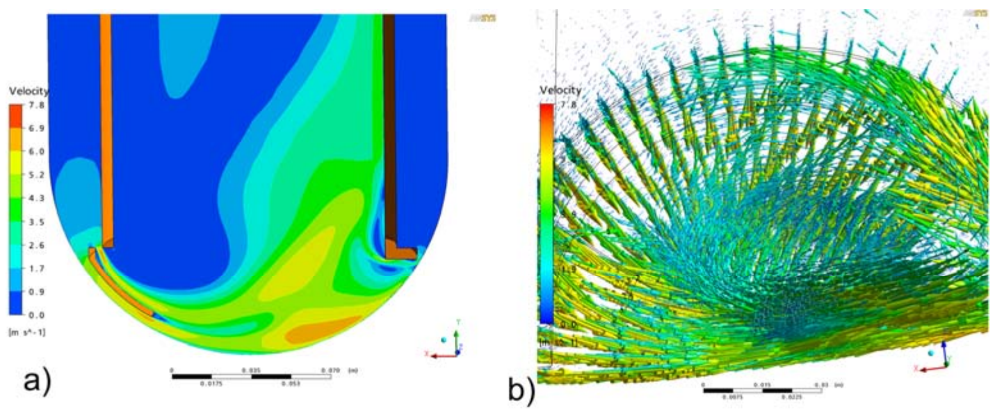

Fig. 5. Zoomed flow field details. a) velocity contour map in the symmetry plane reveals mixing layer, the stagnation zones and the small detachment region near the wall, b) velocity vectors in 3D view from the top reveal how coolant from the annulus flows move away upward towards the target axis.

4. Experimental installation

The experimental installation (Fig. 6) for the LIMET water experiment has been designed and fabricated at PSI. The installation is placed in WMHA (PSI), in the pit of the former test stand for the MEGAPIE target integral test. The installation is assembled in a dark chamber (pos.1, no cover on the picture) fabricated from wooden blocks. A metallic frame (pos.3) is fixed on a very stable concrete wall of the pit (pos.2). The BEW mock-up and two manipulators for the laser and camera (pos.4, pos.9, pos.10) are fixed on the frame. The mock-up inlet and outlet (pos.5 and pos.6) are connected with metallic pipes (DN80, pos. 7 and pos.8) to a water loop (beyond the picture bounds).

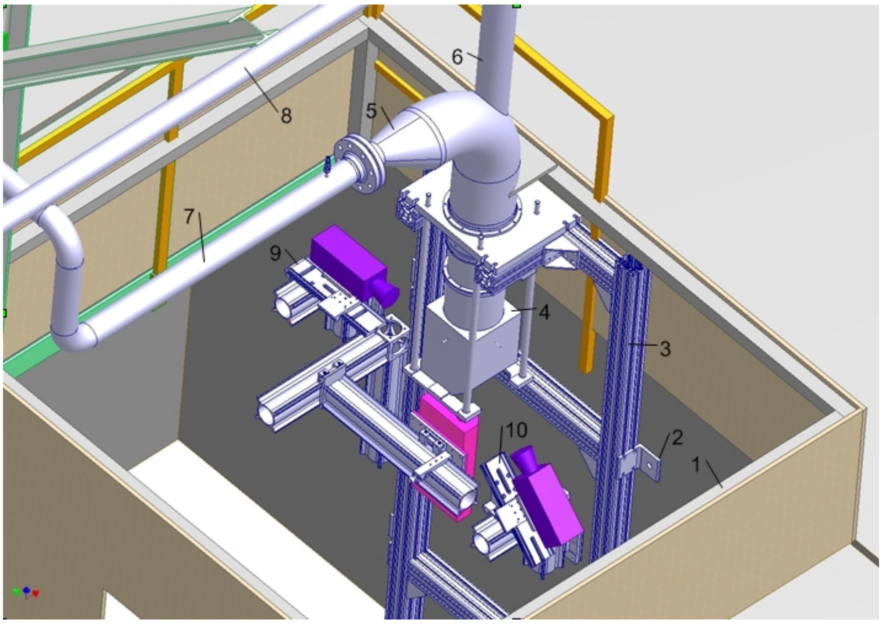

Fig. 6. Set-up of the BEW mock-up in dark chamber: 1 – dark chamber; 2 – wall; 3 - frame; 4 – BEW mock-up; 5 and 6 – inlet and outlet of the mock-up; 7 and 8 – pipes connecting the mock-up with water loop; 9 – manipulator with laser; 10 – manipulator with camera.

The BEW mock-up was designed and fabricated at PSI (Fig. 6 and Fig. 2). Special requirements connected with the PIV set-up were considered during the design process.

- The BEW (pos. 1 in 2) is fabricated from Plexiglas; it is transparent for the laser beam (PIV);
- The riser tube lower part (pos. 3 in Fig. 2) is replaceable; therefore, it is possible to test with different flow geometries;
- The possibility to rotate the riser around the vertical axis without draining of the loop has been provided. This allows quick adjusting of the PIV arrangement for the measurements in different vertical cross-sections of the BEW;
- The flow straighter (honeycomb, not shown in Fig.6) is installed before the riser tube end. Inlet boundary conditions are to be experimentally determined.

5. Measuring and data acquisition system

The instrumentation used for hydraulic and structural test included the following:

- two (first one at the inlet and second one at the outlet) industrial K-type thermocouples (sensitivity 41µV/°C, sheath material AISI 304L, diameter 1-2 mm, and maximum working temperature 900°C) are used for water temperature measurements;
- an industrial flow meter ENDRESS-HAUSER PROWIRL 77 (type 77FS50 – EA011A03; output 4…20mA) is used for measuring total water flow rate in the loop;
- a differential manometer (Rosemount, No.667600; 0 – 350mbar; output 4 – 20mA) is used for total pressure loss measurements in the BEW;

- cover gas pressure is measured with manometer (BACHOFEN UDS7 0427-476; serial No.k213584/004; 18-32VDC; 2bar/4bar; 4-20mA);
- two KISTLER acceleration sensors of type 8632C5 (single axis linear; ±5g; sensitivity 1000mV/g; frequency range 1 to 3000Hz) are used for measuring structural acceleration of the mock-up at two perpendicular locations 250 mm on the riser end;
- a KISTLER pressure sensor (KISTLER 601 connected to amplifier 5011) was used for measuring pressure fluctuations near BEW.

The velocity fields, which are to be used for code validation, are obtained by using a standard, commercial PIV system. It consists of dual cavity lasers and a CCD (Charge Coupled Device) camera that works in a two-frame double exposure mode. The laser light sheet illuminates the mid plane of the flow field, while the camera looks perpendicularly or under defined angle on the laser light sheet. A special dosing system should be used for feeding the flow with seeding particles. More details about PIV systems, their components, the experimental technique in general, main principles and measurement accuracy can be found in many literature sources.

6. First experimental results

6.1. Structural acceleration and pressure measurements

The acceleration and pressure data were collected for no-flow and various flow rates (5, 7 and 9 l/s). As structural acceleration data carry information on coupled fluid-structure interactions, the main objectives are

- to detect indirectly the existence of large coherent structures (instabilities), which affect the structural behavior;
- to detect any kind of resonance occurring during operation of the mock-up;
- to check the system integrity by comparing the signal characteristics for various flow conditions including no-flow;
- to investigate patterns in the frequency domain in case of fully developed turbulent flow.

Experimental results recorded during a standard test are shown in Fig. 7. Structural acceleration, pressure and flow rate data are continually recorded in a database. They cover several steady states and transient regimes. Most interesting outcomes can be summarized below:

- the maximum flow rate investigated was about 9 l/s, whereas the pressure loss in the lower part for Configuration B without turbulent promoter was about 350 mbar;
- the configuration B worked with little structural vibration;
- no resonance frequencies have been detected in the system apart from some tones at high frequencies;
- rms-values of the pressure data were increased four times when the total flow rate was increased from 5 to 9 l/s. The normalized relative frequency distribution of pressure fluctuation is Gaussian as shown in Fig. 7 for all investigated steady states;
- the pressure loss in the target BEW is relatively high; if the same local velocities are to be achieved during the liquid metal test, the pressure loss will be ten times

higher than for the water test for the same geometry. Therefore, the lower target design must be improved and optimized by using CFD tools;

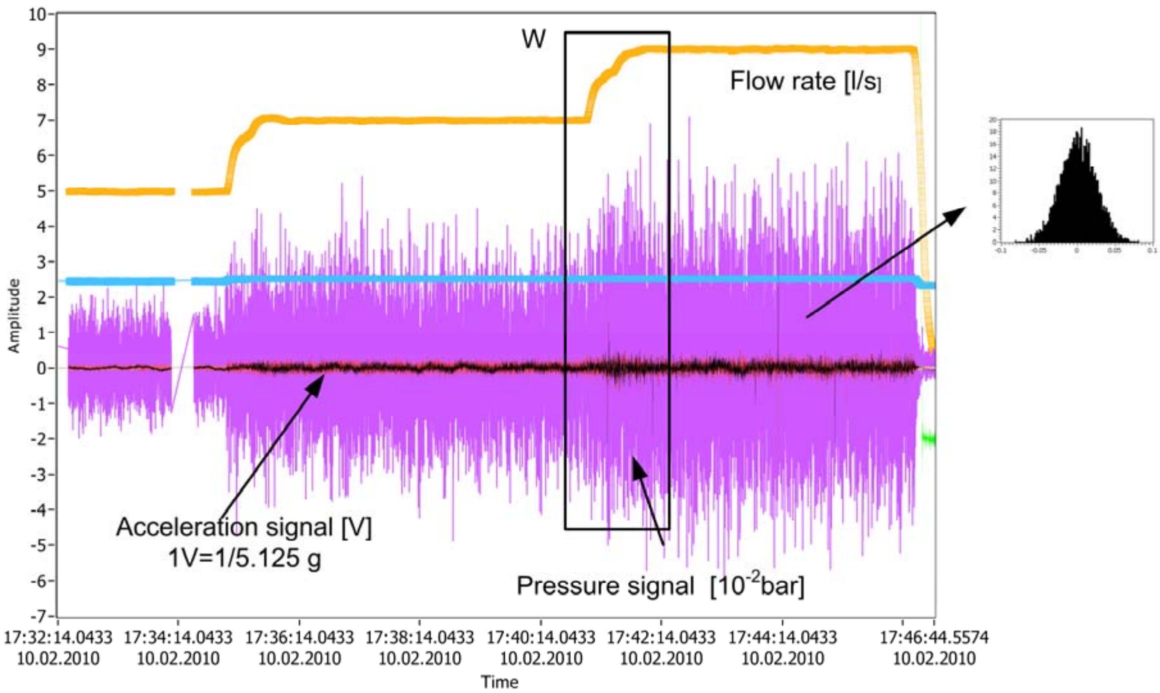

Fig. 7. An overview of data collected during a hydraulic test. An interesting system behavior is registered at high flow rates. Data set of interest is marked by window W. The normalized relative frequency distribution of pressure fluctuation is shown on the left side.

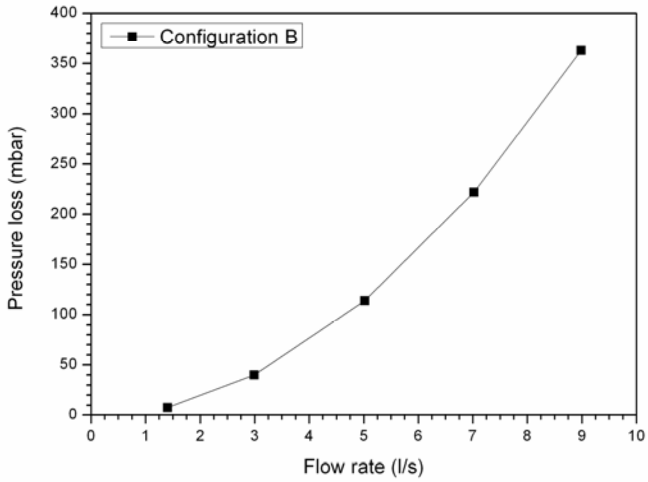

Fig. 8. Pressure loss in the target mock-up

6.2. PIV measurements

PIV measurements in a vertical plane crossing the centre of the riser provided the instantaneous and time- and space- averaged velocity fields. Prior to presenting first experimental PIV velocity fields, some considerations have to be made about the information contained in PIV measurements in relation to the data analysis and interpretation. In the next chapter the basic principles of PIV are briefly explained.

6.2.1. Basic principle of PIV

Two consecutive images that contain light emitted from the fluorescent particles is acquired with the CCD camera. The main idea is to estimate the average particle displacements ($\Delta x, \Delta y$) in small areas of the images called interrogation areas (IA) by cross-correlation techniques. Since the time shift between images corresponds to the time between two laser shots (Δt_{las}), the two velocity components can be calculated as: $U = \Delta x / \Delta t_{las}$; $V = \Delta y / \Delta t_{las}$.

Therefore, after dividing both images into small interrogation areas, the following PIV analyzing algorithm is applied:

1) Filters called window functions manipulate the image gray-scale values and therefore act as input filters to the FFT (Fast Fourier Transform) algorithm. The window functions are suitable weighting functions (Top-hat, Gaussian and etc.). Depending on the pixel position in the IA, the recorded intensity is multiplied with a factor between 0 and 1. Application of these filters allows one to suppress so-called phantom particles and phantom correlations near the edges of the IA;

2) In order to efficiently compute cross-correlations for each IA, the gray-scale image intensity fields are transformed by the FFT algorithm into the frequency spectrum of the gray-intensity distribution;

3) In order to estimate the average particle displacement, the cross-correlation function is calculated for each IA. This function statistically measures the degree of match between two corresponding IA pictures for a given shift. The position of the highest value in the correlation plane is used as the final estimate of the average particle displacement. The space-averaged horizontal and vertical velocity components are obtained by dividing the horizontal and vertical average particle displacement by the time between two laser shots. In general, these results represent time- and space-filtered quantities. The PIV technique applies a spatial low-pass filter to the data, and therefore statistical quantities such as time-averaged mean velocities and stress terms, which are extracted from such PIV data, must be carefully examined.

6.2.2. Experimental versus computational results

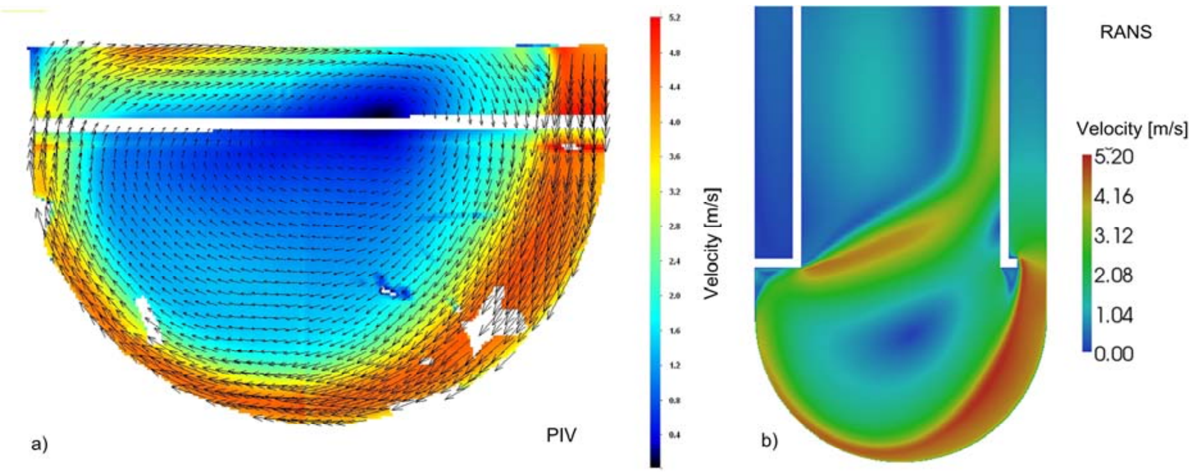

Fig. 9. Scalar maps of the a) PIV time-averaged velocity field (only every forth vector is shown) and b) RANS time averaged velocity field. Data are shown for configuration A and total liquid flow rate of 5 l/s. No PIV data are available for the empty white regions, since they contain laser light reflections. The same colour scale is used for both maps.

Fig. 9 shows a time-averaged velocity field obtained by PIV for comparison with a time-averaged velocity field calculated with RANS method and standard $k-\varepsilon$ model. The PIV velocity field was obtained by superposition of many instantaneous fields. Stagnation regions as well as the jet region near the BEW are well resolved by RANS by using the standard code settings. Several mesh refinements near the wall have been tested.

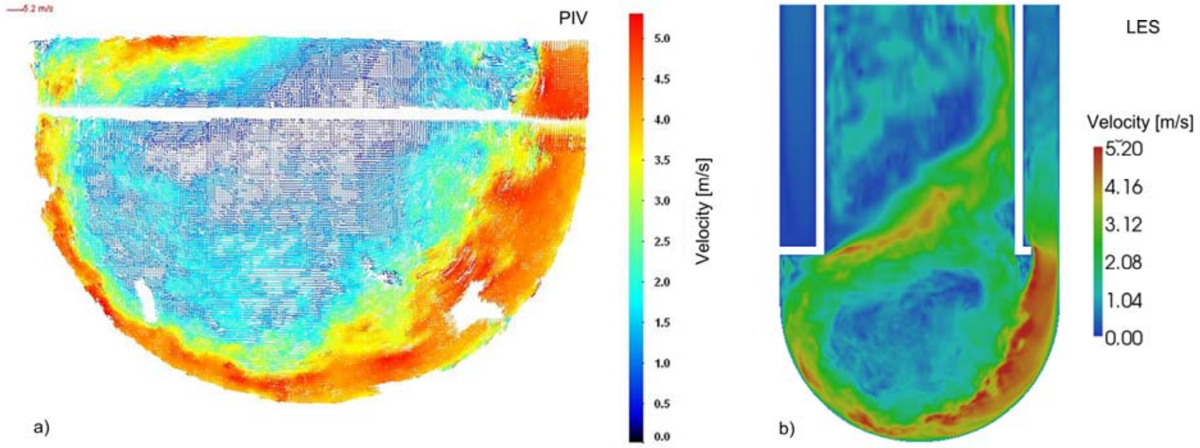

Fig. 10. Scalar maps of the a) PIV instantaneous velocity field (2 velocity components) and b) LES instantaneous velocity field (three velocity components). Data are shown for configuration A and total liquid flow rate of 5 l/s. No PIV data are available for the empty white regions, since they contain laser light reflections. The same colour scale is used for both maps.

Both LES and PIV instantaneous fields (Fig. 10) reveal instabilities in the shear layer, which may cause fluid-induced vibrations of the riser end. Structural vibrations measured during the first water tests were negligible (see Fig. 7).

7. Conclusions

LIMET-a test bed for liquid metal targets is a unique experimental installation developed at PSI for extensive studies of the most important hydrodynamic and structural characteristics for various configurations of the lower end of liquid-metal target prototype. It can however be used for water-cooled solid target development as well.

The experimental investigation provided structural acceleration, pressure and velocity fields, which are used for validating computational methods such as RANS and LES. The first experimental findings are that the cross section of the annulus should be asymmetrically closed. This can provide a jet like stream for cooling the window. By modifying the lower riser end as shown in Fig. 4, the second stream can be used to remove a huge stagnation region shown in Fig. 9. These modifications are to be performed by employing various computational methods and codes. Finally, configurations that provide satisfactory cooling conditions of the BEW are to be tested with liquid metal as working fluid.

The time-dependent and instantaneous structural and hydraulic measurements collected in these experiments form a valuable and consistent database for the validation and development of advanced three-dimensional flow simulation tools as well as reference for developing unique configurations of the BEW and lower riser end.

References

[1] T. Dury, CFD design support at PSI for the international MEGAPIE liquid-metal spallation target, Journal of nuclear science and technology, Vol. 41, No. 3, pp.285-295 2004.
[2] Munson, Young, Okishi, Fundamentals of Fluid Mechanics, 5th Edition, 2006.
[3] ANSYS Inc., ANSYS CFX Solver Modeling Guide, CFX 11.0, 2007.
[3] I. Platnieks, Heat transfer intensification at the proton beam window by creation flow structures containing small scale turbulence in the circumfluent flow, Report, 2009.